ELSEVIER

Journal of Electron Spectroscopy and Related Phenomena 98–99 (1999) 139–148

JOURNAL OF ELECTRON SPECTROSCOPY and Related Phenomena

# The interaction between vapor-deposited Al atoms and methylester-terminated self-assembled monolayers studied by time-of-flight secondary ion mass spectrometry, X-ray photoelectron spectroscopy and infrared reflectance spectroscopy

G.L. Fisher[a], A. Hooper[a], R.L. Opila[b], D.R. Jung[c], D.L. Allara[a], N. Winograd[a]

[a]*Department of Chemistry, The Pennsylvania State University, 152 Davey Laboratory, University Park, PA 16802, USA*
[b]*Lucent Technologies/AT&T Bell Laboratories, 700 Mountain Avenue, Murray Hill, NJ 07974, USA*
[c]*National Renewable Energy Laboratory (NREL), 1617 Cole Boulevard, Golden, CO 80401, USA*

Received 16 October 1997; accepted 27 January 1998

**Abstract**

The deposition of 2 Å of Al metal onto a monolayer of methylester-terminated alkanethiolate ($HS(CH_2)_{15}CO_2CH_3$) self-assembled on polycrystalline Au(111) was studied using time-of-flight secondary ion mass spectrometry (ToF-SIMS), X-ray photoelectron spectroscopy (XPS) and infrared reflectance spectroscopy (IRS). The deposited Al was found to be highly reactive with the oxygen atoms in the self-assembled monolayer terminal functional group. No reactivity between Al and the methylene backbone of the monolayer was observed, nor was any Al observed at the monolayer/Au interface. However, the deposition of Al does induce some chain disordering. 

*Keywords:* Monolayer; Metal deposition; Time-of-flight; Overlayer; Infrared

## 1. Introduction

Self-assembled monolayers (SAMs) formed on metal and semiconductor substrates provide a unique opportunity to study clean, well-characterized organic surfaces [1–3]. By changing the composition of the headgroup, tailgroup and/or backbone of the absorbed molecules, electrical and optical properties may be controlled at the molecular level [1–4]. Some recent studies have focused on depositing metal atoms onto the surface of a molecular monolayer affecting characteristics such as electrical response [5–16]. Many different metals, including Al, Cu, Ag, Cr and Ti, were evaporated onto ω-functionalized monolayers that contain methyl, alcohol, acid, methylester, nitrile and amino functional groups [5–16]. Some metals are observed to bind at the exposed surface of the monolayer while others penetrate into the film [5]. The outcome is dependent upon the metal used and the nature of the terminal organic functional group.

Presently, it is not clear to what extent metal forms a uniform overlayer on the SAM or, conversely, to what extent metal penetrates to the SAM/substrate interface. Ion scattering spectroscopy (ISS) and X-ray photoelectron spectroscopy (XPS) were employed to characterize uniformity and detect penetration of metals through the organic monolayer [5–16]. It was not yet possible, due to the nature of the characterization techniques employed, to disentangle the role of inherent surface defects from thermodynamic

0368-2048/99/$ - see front matter 
PII: S0368-2048(98)00283-7

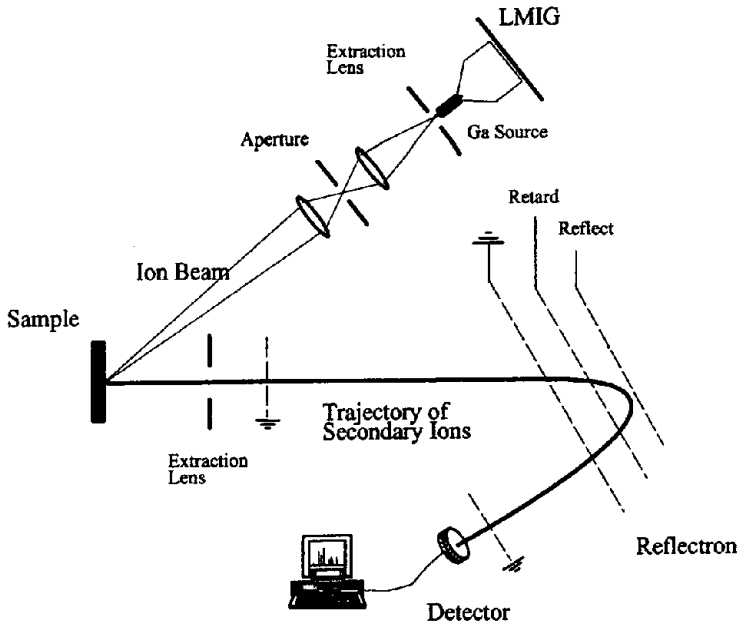


Fig. 1. Schematic diagram of the ToF-SIMS apparatus.

forces and chemical reactions upon deposition. There were a number of proposed applications for metal/SAM systems, including active layers, passive layers and compliant linkages in organic/inorganic composite devices, driving the need for more detailed molecular-level information [4,17–25].

Characterization of organic monolayer surfaces was quite challenging because of the diverse chemistry associated with these systems. Methods such as ellipsometry, XPS, ISS, atomic force microscopy (AFM), scanning tunneling microscopy (STM) and infrared reflectance spectroscopy (IRS) have provided much chemical and structural information but generally lack the specificity required to distinguish between subtle chemical configurations [1,3,5]. Recently, time-of-flight secondary ion mass spectrometry (ToF-SIMS) was employed to examine a variety of ω-functionalized alkanethiolate monolayers and other functionalized organic surfaces [26–37]. In these experiments, many different molecular cluster ions were observed in the mass spectra. Of special chemical interest is the observation of mass peaks associated with units of the intact adsorbate molecules. Moreover, fragment ions associated with the terminal organic functional groups can provide direct information about the chemical state of the molecular surface. Hence, ToF-SIMS offers a unique complementary method to other more developed tools when more detailed chemical information is needed.

In this work we examine the chemical state of a methylester-terminated alkanethiolate monolayer bound to Au, prior to and following room temperature deposition of Al. To obtain as much information as possible about this system, we have employed ToF-SIMS, XPS and IRS to monitor the fate of Al atoms as they react with organic functional groups at the monolayer surface. Although no previous work was published regarding this system, related experiments on polymer surfaces suggest that the Al should react quickly, binding with oxygen-containing organic functional groups at the SAM surface [38–41]. In addition, the possibility exists that Al will penetrate to the SAM/substrate interface [5]. Our results indicate that at sub-monolayer coverages the Al binds only at oxygen sites of the methylester terminus forming a uniform overlayer. As the deposition progresses and the oxygen sites are consumed, small metal islands form on top of the monolayer. Furthermore, our studies indicate that neither does Al does not penetrate to the SAM/substrate interface, nor is there a significant reaction of Al with the methylene backbone of the SAM.

## 2. Experimental

### 2.1. Sample preparation

The preparation and characterization of methylester-terminated SAMs was described in detail previously [42,43]. Briefly, the Au substrates were prepared on native oxide covered Si(001) wafers using a Cr adhesion layer. The Au layer, 2000 Å thick, was evaporated from a resistively heated $Al_2O_3$-coated W-boat and the Cr layer, 100 Å thick, was evaporated from a resistively heated Cr/W-rod. The metals, purchased from Goodfellow and R.D. Mathis, respectively, had purities ≥99.99%. Self-assembly was performed by immersing the Au substrates into millimolar thiol solutions in absolute ethanol for 4 days. The films were characterized with ellipsometry, infrared spectroscopy and contact angle measurements to ensure that they were densely packed and well-ordered. Bare Au reference samples were peroxide-etched and UV-ozone cleaned.

### 2.2. ToF-SIMS

The ToF-SIMS analysis was performed on a custom designed instrument [44]. This instrument consists of a loadlock, a preparation chamber and a primary analysis chamber, each separated by a gate valve. The primary ions are delivered using a $Ga^+$ liquid metal ion gun (LMIG). The primary ion beam is accelerated to 25 keV and has a probe diameter of 100 nm. The secondary ions are focused into a flight tube by an extraction lens.Then,they drift through a field-free region and into a two-stage reflectron where they are time compressed. Lastly, they drift through a second field-free region and strike the multi-channel plate (MCP) detector (Fig. 1). During data acquisition the beam is pulsed with a width of 40 ns at 3 nA and is rastered over a 1600 × 1600 $\mu m^2$ area. All spectra were acquired using a total ion dose of less than $10^{11}$ ions/$cm^2$. Aluminum deposition was carried out in the preparation chamber, using a W-wire basket source, at a rate of 0.1 Å per second. Deposition measurements were made using a Sycon STM-100 quartz crystal microbalance (QCM) controller. Monolayer coverage is defined as 0.75 Å of deposited Al, measured with a QCM assuming a unity sticking coefficient, corresponding to a one-to-one ratio of Al to methylester [2,42]. The pressure remained below 8 × $10^{-8}$ torr during deposition. The base pressure of the system was 1.5 × $10^{-9}$ torr which was recovered before sample transfer.

### 2.3. XPS

The XPS analysis was performed on a Scienta ESCA 3000 spectrometer equipped with a monochromatic Al K$\alpha$ source and is described in detail elsewhere [45,46]. A pass energy of 75 eV and an energy step of 0.05 eV was used for the analysis. The resulting full-width at half-maximum (FWHM) for Au $4f_{7/2}$ was found to be 0.52 eV. A binding energy of 84.0 eV for Au $4f_{7/2}$ was used as a reference for all spectra.

Following initial XPS analysis of the SAM, the sample was transferred under vacuum to the aluminum evaporation chamber, which was isolated from the analysis chamber by a gate valve. The pressure in the preparation chamber remained below 1 × $10^{-8}$ torr during deposition. Incremental amounts of Al were deposited at a rate of 1.0 Å per minute by evaporation from a graphite crucible heated to 975°C. The deposition rate was checked periodically by removing a check sample and analyzing with Rutherford backscattering spectroscopy. The Al/SAM specimen was transferred without exposure to air to the analysis chamber.

### 2.4. IRS

IRS analysis was performed on a Mattson Research Series instrument with custom optics optimized for grazing incidence reflection. A liquid nitrogen cooled mercury-cadmium-telluride (MCT) detector was used with an effective frequency range of ~ 750–8000 $cm^{-1}$. The infrared beam was allowed to access the vacuum system and reflect from the sample through a pair of differentially-pumped KBr windows. All of the FTIR optics and electronics were positioned outside the vacuum system with only the infrared beam entering the vacuum chamber. This scheme allowed Al deposition and FTIR analysis to be performed without moving the sample. After analysis of the clean methylester SAM, a shield was opened between the sample and the Al source. The Al was evaporated from a W-wire basket at a rate of 1.0 Å per

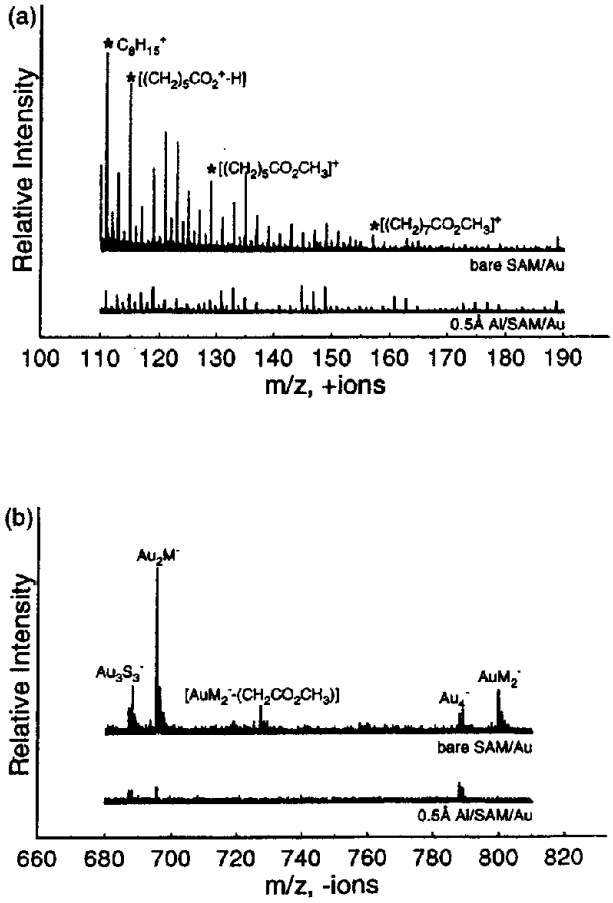


Fig. 2. SIMS spectrum of methylester-terminated SAM before and after deposition of 0.5 Å Al. (a) Positive ions. (b) Negative ions.

minute measured by the QCM. The pressure remained below $1 \times 10^{-7}$ torr during the deposition.

## 3. Results and discussion

We have combined the techniques of ToF-SIMS, XPS and IRS in order to develop a more complete understanding of the chemical bonds formed when Al is deposited onto a methylester-terminated SAM. Our strategy was to acquire high quality reference spectra from the virgin methylester-terminated surface and follow changes in the spectra as increasing amounts of Al were deposited. Of particular interest was the observation of changes in the intensity of SIMS cluster ions involving O and Al. The observed changes in the mass spectra were compared to XPS and IRS data at corresponding Al coverages.

### 3.1. ToF-SIMS

The ToF-SIMS spectra for both positive and negative ions are shown in Fig. 2. The peak intensities are reproducible to within ± 5%, from sample to sample. In general, we find that the relative intensities of the $Au_x$ and $Au_xS_y$ cluster ions provide a useful indication that the sample was prepared without impurities or oxidative products. These cluster ion intensities are close to those observed previously for ToF-SIMS spectra of other SAMs [26,27]. The information associated with the positive ion spectrum is mostly found below a mass-to-charge ratio ($m/z$) of 200, and no molecular ion signal is observed. The negative ion

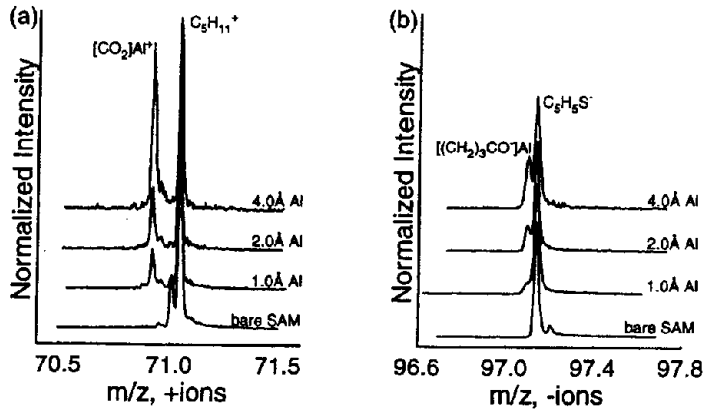


Fig. 3. (a) 1.0 amu window following progression of the $[CO_2]Al^+$ metal-organic fragment with Al deposition. (b) 1.0 amu window following progression of the $[(CH_2)_3CO^-]Al$ metal-organic fragment with Al deposition.

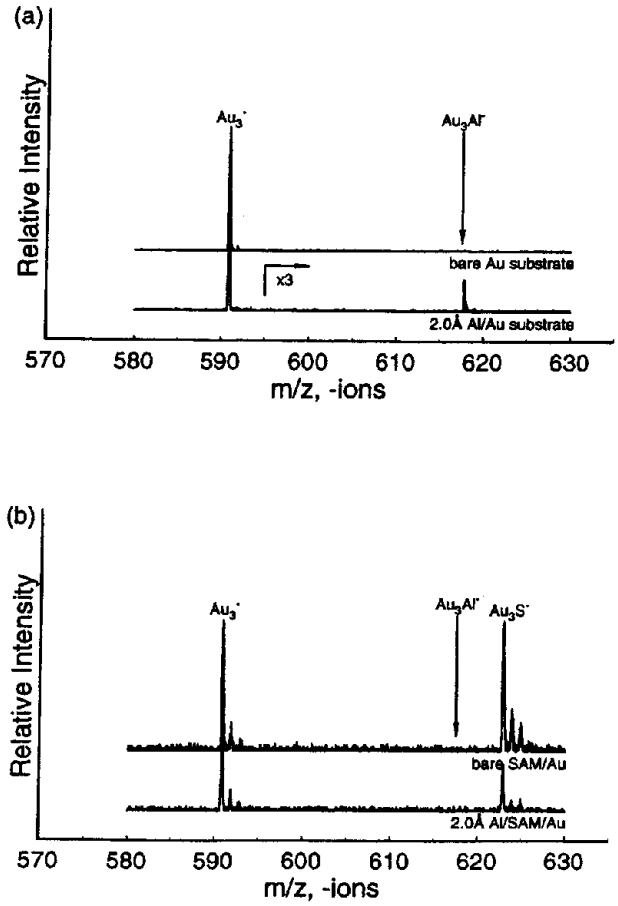


Fig. 4. (a) Negative ion spectrum of bare Au reference and the same reference after deposition of 2.0 Å Al. (b) Negative ion spectrum of bare methylester-terminated SAM before and after deposition of 2.0 Å Al.

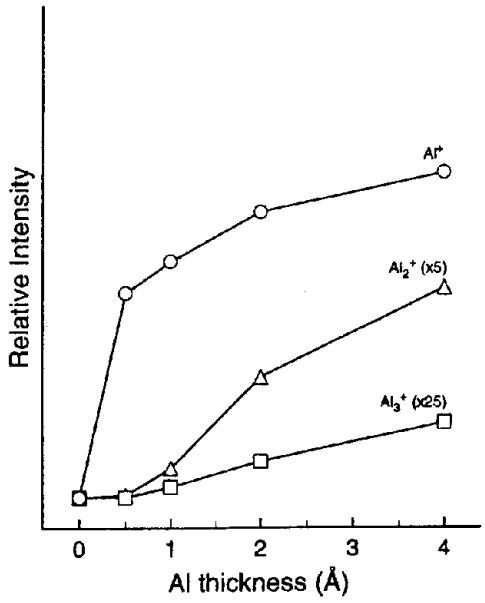


Fig. 5. Al monomer, dimer and trimer intensity versus overlayer thickness.

spectrum, however, reveals a number of cluster ions that contain intact adsorbate molecules at *m/z* = 670–820. No metal-carbide species were observed in the mass spectra.

It is feasible to assign most of the important mass peaks shown in Fig. 2. The positive ion spectrum contains a series involving methylester-terminated moieties, such as $[(CH_2)_xCO_2CH_3]^+$ and $[(CH_2)_xCO_2]^+$ where $x = 3$, 4 and 5. Other fragments of interest are $C_5H_{11}^+$ at *m/z* = 71.09, $(CH_2)_{14}CO^+$ at *m/z* = 224.22 and $S(CH_2)_{15}^+$ at *m/z* = 242.21, but are not shown in Fig. 2. The negative ion spectrum exhibits a number of high mass peaks that involve the intact molecular ion of the methylester-terminated alkanethiolate $M{=}S(CH_2)_{15}CO_2CH_3$, as well as a number of important fragment ions. The mass peaks involving molecular ions are $AuMH^-$ at *m/z* = 449.19, $Au_2M^-$ at *m/z* = 695.14, $Au(M_2 - CH_2CO_2CH_3)$ at *m/z* = 726.38 and $AuM_2^-$ at *m/z* = 799.41. The mass peaks involving fragment ions are $CH_2CO_2CH_3^-$ at *m/z* = 73.03, $C_4H_4CO^-$ at *m/z* = 80.03 and $C_5H_5S^-$ at *m/z* = 97.01. Negative ions in the mass range 680 to 810 are shown in Fig. 2.

The next series of experiments involved deposition of Al onto the SAM surface and noting changes in the aforementioned mass peaks, as well as the appearance of new features involving Al. A prominent feature of the spectra in Fig. 2 is the rapid disappearance of oxygen-containing fragments at sub-monolayer coverages of Al, although there still remain a number of aliphatic hydrocarbon peaks. As the deposition progresses these peaks eventually disappear, along with the metal-organic fragment peaks, as a result of attenuation from Al overlayers. This effect is illustrated in greater detail in Fig. 3. Here, we follow metal-organic fragment peak intensities with Al deposition within a window of one mass unit. These spectra are interesting because the fragments in each window have nominal masses of 71 and 97 amu, respectively. However, the high mass resolution of ToF-SIMS allows these isobaric fragments to be readily separated. The spectra are normalized to the initial peak intensities of $C_5H_{11}^+$ and $C_5H_5S^-$ to make obvious the increasing intensity of the metal-organic fragments with respect to the hydrocarbon fragments. In reality, the metal-organic fragments reach maximum intensity between 1.0 and 2.0 Å of deposited Al, then begin to decrease in intensity due to the thickening of Al overlayer. These data clearly suggest that the Al atoms interact directly with the oxygen-containing functional groups of the organic monolayer.

It is possible to determine whether significant numbers of Al atoms are penetrating the monolayer film and binding directly to the Au surface. We have compared the spectrum of Al deposited onto a bare Au reference with that of Al deposited onto methylester-terminated SAM as shown in Fig. 4. The reference spectra reveal which $Au_xAl_y$ clusters would appear in the positive and negative spectra as a positive test of Al penetration to the SAM/substrate interface. No $Au_xAl_y$ cluster peaks were found in the Al/SAM/Au spectra, indicating that Al does not significantly penetrate to the SAM/substrate interface.

Information regarding Al overlayer uniformity may be deduced from an intensity versus coverage plot for monomer, dimer and trimer species as shown in Fig. 5. At sub-monolayer coverage, the monomer signal dominates, whereas the dimer and trimer signals are not observable. As the deposition proceeds the dimer and trimer intensities increase, reaching appreciable levels only after 2.0 Å of Al were deposited. Collision-induced dimer formation requires a monomer

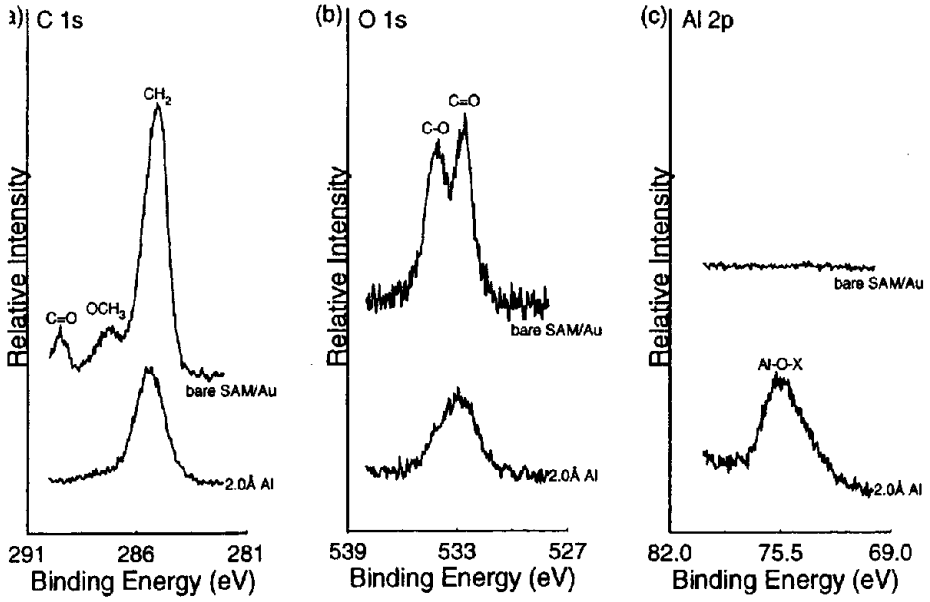


Fig. 6. The core-level spectra of a methylester-terminated SAM before and after the evaporation of 2.0 Å Al. (a) The C 1s core-level spectra. (b) The O ls core-level spectra. (c) The Al 2p core-level spectra. All spectra were taken at 10° take-off angle.

separation of no more than 5 Å [47]. The van der Waals radius of a methylester-terminated SAM is approximately 3.4 Å placing Al atoms well within the range for dimer/trimer formation, even at low coverage, following collision-induced ejection [1,3,42,43]. The data indicate that, at sub-monolayer coverage, the Al overlayer is uniform. If Al clusters were formed at sub-monolayer coverage they would appear in the mass spectra. However, only after the oxygen-containing groups were consumed do islands begin to form, yielding dimers and trimers in the mass spectra. We may also conclude that, at sub-monolayer coverages, Al diffuses across the surface of methylester-terminated SAM binding tightly to the oxygen-containing groups. Finally, the lack of collision-induced dimers in the mass spectra at sub-monolayer coverage suggests that the Al—O bond is quite strong.

### 3.2. XPS

Chemical information obtained by ToF-SIMS are supported by the XPS data Core-level shifts for C 1s, O 1s and Al 2p before and after the application of 2.0 Å Al to the methylester-terminated SAM is shown in Fig. 6. Improved signal-to-noise ratio and surface selectivity was obtained by using a 10° take-off angel. Peak areas and energies were determined by curve-fitting, using a mixed 90% Gaussion/10% Lorentzian shape (with the notable exception of the Au 4f peaks which had a larger Lorentzian component). The spectra were all shifted so that the Au $4f_{7/2}$ energy was at exactly 84.0 eV. The binding energies of the bare methylester-terminated SAM agree with those previously reported [9].

The spectra of this monolayer shows four types of carbon atoms that were assigned as follows: (1) $CH_2$ for the alkyl chain at 284.89 eV; (2) $-CH_2-COO-$ carbon in the $\alpha$ position for the carbonyl carbon at 285.96 eV (this peak appears as a shoulder on the $CH_2$ peak and is resolved by curve-fitting); (3) $-OCH_3$ methoxy carbon at 287.28 eV; (4) $COO-$ carbonyl carbon at 289.35 eV. There are two peak assignments made for the O 1s spectra: the peak at 532.57 eV was assigned to the C=O oxygen, and the peak at 534.12 eV was assigned to the $-OCH_3$ oxygen.

Following Al deposition the chemical shifts are noticeably altered. Examination of the C 1s XPS spectra in Fig. 6(a) shows a complete loss of the two higher binding energy peaks associated with the C=O

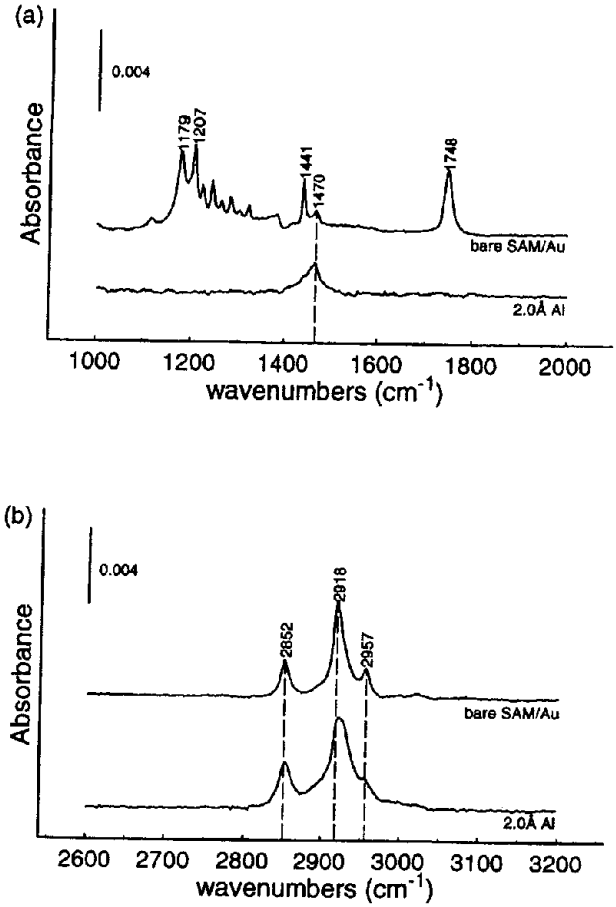


Fig. 7. Infrared reflectance spectra for a methylester-terminated SAM before and after deposition of 2.0 Å Al. (a) Low frequency region. (b) High frequency region.

and C—O species. The size of the $CH_2$ core level shift associated with the methylene chain has decreased in area and has broadened. The reduced size of the methylene peak is more likely due to attenuation of the signal by the Al overlayer. No peak associated with the formation of aluminum carbide is observed (expected at 282.3 eV)

Examination of the O 1s XPS spectra in Fig. 6(b) shows that the two peaks associated with the C=O and C—O oxygen atoms are replaced with a single, broad peak. Loss of the carbonyl and methoxy C 1s peaks, mentioned above, suggests that this broad oxygen peak is more likely due to formation of Al—O—C species. Likewise, analysis of the Al 2p XPS spectra in Fig. 6(c) shows the obvious appearance of an aluminum oxide peak. The unexposed SAM demonstrates that the observed peak results from the Al species, and is not an artefact from the Au substrate (the Au 5p core level shift occurs at 74 eV). The observed Al 2p peak is very broad and is centered at 75.4 eV. The shape of the peak suggests that there are lower energy components present. Metallic Al has a 2p core level shift at 72.8 eV, and the appearance of the peak at 75.4 eV suggests that most of the evaporated aluminum forms Al—O—C species.

### 3.3. IRS

The IRS spectra of the methylester-terminated SAM, before and after Al deposition, is shown in Fig. 7. The series of sharp bands between ~ 1200 and 1350 $cm^{-1}$ are assigned to the progression of $CH_2$

twisting and wagging modes. The presence of these bands indicates that the SAM is in an all-*trans* conformation with very few *gauche* defects. The two peaks at 1179 and 1207 $cm^{-1}$,respectively, correspond to the C—O stretching modes. The peak at 1441 $cm^{-1}$ corresponds to the $CH_3$ symmetric bend in the methoxy group. The peak at 1470 $cm^{-1}$ corresponds to the $CH_2$ scissor mode of the methylene groups in the backbone. The peak at 1748 $cm^{-1}$ corresponds to the carbonyl (C=O) stretching mode. The high frequency region shows peaks at 2852 and 2918 $cm^{-1}$ corresponding to $CH_2$ symmetric and antisymmetric stretches, respectively. Finally, the peak at 2957 $cm^{-1}$ is assigned to the $CH_3$ asymmetric stretching mode of the methoxy group. These peak assignments were made previously [43].

The peaks associated with the ester C=O and C—O stretching modes are removed by 2.0 Å Al exposure indicating chemical disruption of the methylester group. Both of the $CH_2$ stretching modes at 2852 $cm^{-1}$ and 2918 $cm^{-1}$ were considerably broadened, indicating some disorder. In agreement with this conclusion, the symmetric and antisymmetric stretches were shifted up by 1 $cm^{-1}$ and 6 $cm^{-1}$, respectively. The peak at 1470 $cm^{-1}$ also remains, indicating a fully intact methylene backbone. Finally, asymmetric methyl stretch and symmetric methoxy bend are still present at 2957 $cm^{-1}$ and 1441 $cm^{-1}$, respectively. These peaks are attenuated but indicate the presence of intact $-O-CH_3$ in the methylester group.

## 4. Conclusions

Our experiments consistently indicate that Al reacts readily with oxygen in the methylester functional group until all oxygen is bound to the deposited Al. This conclusion is supported by the loss of the C—O and C=O peaks in the C 1s XPS data, the loss of the low frequency modes in the FTIR spectra and of oxygen-containing fragments in the mass spectra within the first 2.0 Å of deposited Al. The unshifted, albeit attenuated methyl asymmetric stretch and bending modes at 2957 and 1441 $cm^{-1}$, respectively suggest that Al binds preferentially to the carbonyl (C=O) oxygen. The continued presence of $CH_2$ peaks in the IRS data and the lack of metal-carbide peaks in the ToF-SIMS data are evidence that Al does not react with the methylene backbone of the monolayer or with carbon at the monolayer surface. Deposited Al does not penetrate to the SAM/Au interface and there is little or no Al clustering below 2.0 Å of deposited Al. Finally, deposition of Al induced slight disorder within the SAM. This is reasonable because Al—O—C bonding would eliminate a primary source of intermolecular stabilization. The Al/SAM/Au system provides an excellent model with which to test novel concepts in molecular electronics. The strategy reported here may be employed to analyze other monolayer systems as candidates for composite material applications with equal success.

## Acknowledgements

Financial support for this research was provided by the Office of Naval Research, the National Science Foundation and the National Institutes of Health. N. W. would like to acknowledge a long scientific interaction and personal friendship with C.R. Brundle. These relationships extend back to the Namur meeting on X-ray photoelectron spectroscopy in 1974. The proceedings of that meeting, of course, constituted an important volume for this journal. At that time Brundle was focusing on the use of XPS to characterize metal and metal-oxide surfaces, a topic close to our interests as well. Some of his challenges directly inspired our group to take up the use of ion/solid interactions for surface characterization and to complement XPS measurements, an approach we have been pursuing ever since. I recall a burning issue from those days – whether to plot binding energy from right-to-left of left-to-right. Brundle solved the problem by using both conventions, sometimes in the same lecture.

## References

[1] A. Ulman, Chem. Rev. 96 (1996) 1533.
[2] L.H. Dubois, R.G. Nuzzo, Ann. Rev. Phys. Chem. 43 (1992) 437.
[3] J.D. Swalen, D.L. Allara, J.D. Andrade, E.A. Chandross, S. Garoff, J. Israelachvili, T.J. McCarthy, R. Murray, R.F. Pease, J.F. Rabolt, K.J. Wynne, H. Yu, Langmuir 3 (1987) 932.
[4] A. Kumar, L.A. Nicholas, K. Enoch, H.A. Biebuyck, G.M. Whitesides, Acc. Chem. Res. 28 (1995) 219.

[5] D.R. Jung, A.W. Czanderna, Crit. Rev. Sol. St. Mat. Sci. 19 (1994) 1.
[6] D.R. Jung, A.W. Czanderna, G.C. Herdt, J. Vac. Sci. Tech. A14 (1996) 1779.
[7] A.W. Czanderna, D.E. King, D. Spaulding, J. Vac. Sci. Tech. A9 (1991) 2607.
[8] R. Jung, D.E. King, A.W. Czanderna, J. Vac. Sci. Tech. A11 (1993) 2382.
[9] K. Konstadinidis, P. Zhang, R.L. Opila, D.L. Allara, Surf. Sci. 338 (1995) 300.
[10] M.J. Tarlov, Langmuir 8 (1992) 80.
[11] W.J. Dressick, C.S. Dulcey, J.H. Georger Jr, G.S. Calabrese, J.M. Calvert, J. Electrochem. Soc. 141 (1994) 210.
[12] D.R. Jung, D.E. King, A.E. Czanderna, Appl. Surf. Sci. 70/71 (1993) 127.
[13] G.C. Herdt, A.W. Czanderna, Surf. Sci. Lett. 297 (1993) L109.
[14] Y. Hirose, A. Kahn, V. Aristov, P. Soukiassian, Appl. Phys. Lett. 68 (1996) 217.
[15] G.C. Herdt, D.E. King, A.W. Czanderna, Z. Phys. Chem. 202 (1997) 163.
[16] Mittal, K., Lee, K.-W., 1997, Polymer Surfaces and Interfaces: Characterization, Modification and Applications, VSP International Science Publishers, Netherlands, p. 189-224.
[17] L.A. Bumm, J.J. Arnold, M.T. Cygan, T.D. Dunbar, T.P. Burgin, L. Jones II, D.L. Allara, J.M. Tour, P.S. Weiss, Science 271 (1996) 1705.
[18] L.F. Rozsnyai, M.S. Wrighton, Langmuir 11 (1995) 3913.
[19] M.P. Samanta, W. Tian, S. Datta, J.I. Henderson, C.P. Kubiak, Phys. Rev. B53 (1996) R7626.
[20] S. Rubin, J.T. Chow, J.P. Ferraris, T.A. Zawodzinski Jr, Langmuir 12 (1996) 363.
[21] J.K. Schoer, C.B. Ross, R.M. Crooks, T.S. Corbitt, M.J. Hampden-Smith, Langmuir 10 (1994) 615.
[22] A. Kumar, H.A. Biebuyck, G.M. Whitesides, Langmuir 10 (1994) 1498.
[23] H. Ohno, L.A. Nagahara, S. Gwo, W. Mizutani, H. Tokumoto, Jap. J. Appl. Phys. 35 (1996) L512.
[24] T. Kawai, T. Yamaue, K. Tada, M. Onoda, S.-H. Jin, S.-K. Choi, K. Yoshino, Jap. J. Appl. Phys. 35 (1996) L741.
[25] S.J. Potochnik, P.E. Pehrsson, D.S.Y. Hso, J.M. Calvert, Langmuir 11 (1995) 1841.
[26] M.J. Tarlov, J.G. Newman, Langmuir 8 (1992) 1398.
[27] B. Hagenhoff, A. Benninghoven, J. Spinke, M. Liley, W. Knoll, Langmuir 9 (1993) 1622.
[28] D.A. Offord, C.M. John, J.H. Griffin, Langmuir 10 (1994) 761.
[29] C.D. Frisbie, J.R. Martin, R.R. Duff Jr, M.S. Wrighton, J. Am. Chem. Soc. 114 (1992) 7142.
[30] R. Galera, J.C. Blais, G. Bolbach, Int. J. Mass Spec. Ion Proc. 107 (1991) 531.
[31] B. Hagenhoff, M. Deimel, A. Benninghoven, H.-U. Siegmund, D. Holtkamp, J. Phys. Appl. Phys. D25 (1992) 818.
[32] D.M. Hercules, J. Mol. Struc. 292 (1993) 49.
[33] A.M. Leeson, M.R. Alexander, R.D. Short, D. Briggs, M.J. Hearn, Surf. Int. Anal. 25 (1997) 261.
[34] A.A. Galuska, Surf. Int. Anal. 25 (1997) 1.
[35] M.-L. Abel, M.M. Chehimi, A.M. Brown, S.R. Leadly, J.F. Watts, J. Mater. Chem. 5 (1995) 845.
[36] D. Briggs, I.J. Fletcher, Surf. Int. Anal. 25 (1997) 167.
[37] Wood, M.C., 1995, Surface Characterization and Imaging with Ion-Induced Desorption and Multiphoton Resonance Ionization. Ph.D. Thesis, The Pennsylvania State University, p. 34-111.
[38] M. Bou, J.M. Martin, Th. Le Mogne, Appl. Surf. Sci. 47 (1991) 149.
[39] P. Stoyanov, S. Akhter, J.M. White, Surf. Int. Anal. 15 (1990) 509.
[40] B.M. DeKoven, P.L. Hagans, Appl. Surf. Sci. 27 (1986) 199.
[41] Lj Atanasoska, S.G. Anderson, H.M. Meyer III, L. Zhangda, J.H. Weaver, J. Vac. Sci. Technol. A. 5 (1987) 3325.
[42] P.E. Laibinis, G.M. Whitesides, D.L. Allara, Y.T. Tao, A.N. Parikh, R.G. Nuzzo, J. Am. Chem. Soc. 113 (1991) 7152.
[43] R.G. Nuzzo, L.H. Dubois, D.L. Allara, J. Am. Chem. Soc. 112 (1990) 558.
[44] R.M. Braun, P. Blenkinsopp, S.J. Mullock, C. Corlett, K.F. Willey, J.C. Vickerman, N. Winograd, Rapid Comm. Mass Spec. 12 (1998) 1246.
[45] G. Beamson, D. Briggs, S.F. Davies, I.W. Fletcher, D.T. Clark, J. Howard, U. Gelius, B. Wannberg, P. Balzer, Surf. Int. Anal. 15 (1990) 541.
[46] U. Gelius, B. Wannberg, P. Balzer, H. Fellner-Feldegg, G. Carlsson, C.-G. Johansson, J. Larsson, P. Munger, G. Vegerfors, J. Electron Spec. Rel. Phenom. 52 (1990) 747.
[47] N. Winograd, Mat. Fys. Medd. Dan. Vid. Selsk. 43 (1994) 223.